CFD Letters www.cfdl.issres.net Vol. 5 (4) – December 2013

Effect of Volume Fraction on the Performance and Separation Efficiency of a De-oiling Hydrocyclone

Kamel A. Elshorbagy, Amr Abdelrazek* and Mohamed Elsabaawy

Faculty of Engineering, Alexandria University, Alexandria, EGYPT

Received: 29/07/2013 – Revised 23/09/2013 – Accepted 01/11/2013

Abstract

The flow behaviour in hydro-cyclone is quite complex. The complexity of fluid flow in the cyclone is due to the fact that flow in a cyclone is a swirling turbulent multiphase flow. This paper presents a numerical investigation on the effect of volume fraction (% of phase 2-oil- to the total inlet flow-water + oil-, by volume) on the liquid–liquid hydro-cyclone performance. A mathematical model for the two components of flow is developed using the RNG k-ε model, and employing the Eulerian– Eulerian approach. The flow features were examined in terms of flow field velocity (axial, radial and tangential), pressure drop and separation efficiency. Results indicate that on increasing the volume fraction the static pressure increases, the axial velocity decreases, the radial velocity decreases, and the tangential velocity has almost unaltered. In addition, the separation efficiency is affected by the volume fraction. The increase of volume fraction increases the separation efficiency. However, increasing the volume fraction leads to increase in the separated part of phase 1 (water) and decrease the separated part of phase 2 (oil).

Keywords: Hydrocyclone; CFD; Eulerian- Eulerian; RNG k-ε

1. Introduction

A hydrocyclone is a device to classify, separate or sort particles in a liquid suspension based on the ratio of their centripetal force to fluid resistance. This ratio is high for dense (where separation by density is required) and coarse (where separation by size is required) particles, and low for light and fine particles. Hydrocyclones also find application in the separation of liquids of different densities. The theory and principles of a cyclone is simply that the fluid under pressure is administrated at a tangential inlet to the cyclonic body. The fluid develops a vortex system; an outer vortex moving in the underflow direction and an inner reversed vortex, moving in the overflow direction, [1,2]. The vortex is formed physically in a hydrocyclone due to the swirling motion of the tangentially inlet liquid velocity and resulted in low pressure regime within the cyclone. Thus an air-core is formed. The air comes through the underflow of the hydrocyclone from atmosphere [3]. The swirl intensity is related, by definition, to the local axial and tangential velocities. Therefore, it is assumed that once the swirl intensity is predicted for a specific axial location, it can be used to determine the velocity profiles [4]. On reviewing previous research on hydrocyclones, one may cite Husveg et al. [1] who described the performance of a de-oiling hydrocyclone during variable flow rates, and found that increasing flow rates reduce the pressure drop ratio (PDR). If the PDR reduction is too

* Corresponding author: Amr Abdelrazek
Email: amr_abdelrazek_62@yahoo.com
 PII: S2180-1363(13)54153-X

large, hydrocyclone efficiency drops off. On the other hand, reducing flow rates leads to increase in PDR. An increase in PDR increases the flow split and may marginally increase hydrocyclone efficiency. Hai-fei et al. [5] studied experimentally the oil/water separation in a liquid-liquid cylindrical cyclone. The separation efficiency increases with increasing the flow split-ratio. An appropriate increase of the inlet flow rate can improve the oil/water separation. Through a dimensional analysis, the separation efficiency is a function of the Reynolds number and the flow split-ratio. Hwang et al. [6] studied the improvement of particle separation efficiency in a 20-mm hydrocyclone by installing a conical top-plate. Particle trajectories were simulated based on a Lagrangian frame by considering the interactions with continuous phase, once the fluid velocity distributions become known. Increasing the cone angle decreased the circulation flow and therefore increased the tangential velocity and centrifugal effect near the hydrocyclone wall. The optimum design of the cone angle is 30°. Wang L. and Wang J. [7] saved energy by the so called Reducing Pressure Drop Stick (REPDS), installed in a new hydrocyclone to reduce the pressure drop. The drag reduction of the REPDS increases with increasing the radial position of the REPDS. Amini et al. [8] developed a new mathematical approach for the evaluation of de-oiling hydrocyclone efficiency. The proposed model considered the effects of size distribution of oil droplets, hydrocyclone geometry and flow rate on separation efficiency. Honaker et al. [9] evaluated the benefits of tangential water injection into the apex portion of a classification cyclone for the removal or minimization of the ultrafine by-pass. Parametric effects were studied using empirical models derived from some test data. Quadratic models were used to describe the by-pass and imperfection as a function of two operating and three geometric parameters. The accuracy of predictions were found to be reasonable, as indicated by coefficient of determination values greater than 90%. Swain et al.[10] used the Eulerian–Eulerian CFD simulation approach of a solid–liquid hydrocyclone to study two solid phases and one liquid phase. Two turbulent models, the Reynolds stress model (RSM) and the standard k-ε model were used and they noted that with increase in flow rate, the separation efficiency increased and the separation efficiency predicted by the k-ε model found to be close to that predicted by the RSM model for the low flow rates at which the simulations were carried out. Very fine mesh could not be used as the Eulerian–Eulerian model is computationally intensive and for multiphase systems, it becomes still difficult. Narasimha et al. [11], predicted the flow velocities and air-core diameters using the DRSM (differential Reynolds stress model), LES(large eddy simulation) model and the VOF (volume of fluid) model, for the air phase made analysis for various inlet water velocities and compared their finding with experimental results. The LES turbulence model led to an improved turbulence field prediction and thereby to more accurate pressure and velocity fields. An increase in the viscosity of the liquid reduces the air-core diameter at constant feed velocity by lowering the pressure drop over the cyclone. Bhaskar et al. [12] developed a methodology for simulating the performance of hydrocyclone. Initial work included comparison of experimental and simulated results generated using different turbulence models i.e., standard k-ε, RNG k-ε and RSM in terms of water throughput and split with the help of suitably designed experiments. The simulation results adopting RSM model were found to have better agreement of predictions with experimental results. Parametric results have indicated that the feed inlet pressure has a major influence on mass flow through the cyclone and spigot opening on percent split into the over flow. Yaojun et al. [13] used the Reynolds stress transport equation model to predict the strongly swirling turbulent flows in a liquid-liquid hydrocyclone, and the predictions are compared with LDV measurements. Puprasert et al. [15] investigated the hybrid hydrocyclone process, involving micro-bubbles injection generated by the dissolved air flotation technique. Efficiencies of 61 ± 4% for turbidity decrease and 77 ± 20% for suspended solids removal were obtained. The separation efficiency between the clarified water and the flocs reached 95 ± 10%. This process achieved continuous operation with 1000 L/h inlet flow. Zhao et al. [16] considered the effect of structural type, geometric parameters, and operation parameters on the performance of hydrocyclones. They focused on gas–liquid separation, and numerical simulation of the typical hydrocyclone was carried out. As a 3-phase hydrocyclone, Topcu [17] studied numerically the case

of gas-liquid-solid flow in the cyclone. The turbulent flow of the gas and the liquid modeled using the realizable k-ε model. The air-core development is observed to be a transport effect due to the velocity of surrounding fluid rather than a pressure effect. Shi-Ying et al. [18] reported experimental results on a new vane-type pipe separator (VTPS). The experiments were conducted for the possible application in the well bore for oil–water separation and reinjection. Amini et al. [4] mathematically predicted the efficiency of a down-hole oil–water separation hydrocyclone. In the proposed model, the separation efficiency was determined based on droplet trajectory of a single oil droplet through the continuous-phase. The droplet trajectory model was developed using a Lagrangian approach in which single droplets traced in the continuous-phase. Hualin et al. [19] mentioned the techniques and industrial applications of the reinforced cyclonic separation process. Murthy and Bhaskar [20] investigated numerically and validated with experiments a range of process conditions and provided further understanding on the parametric design and operating conditions. Shu-ling et al. [21] studied numerically the simulation of flow velocity of hydrocyclone conducted with different structural and operational parameters. Distribution characteristics and influencing mechanism were Delgadillo and Rajamani [22] used CFD to numerically predict the hydrodynamic performance for different geometries for the sake of finding the desired classification. Bergström et al. [2] surveyed an overview of the contributions and found that fewer experimental studies investigate the internal flow field and only one study treated the flow as three-dimensional flow. Sripriya et al. [23] studied the separation performance characteristics of the hydrocyclone. They considered the effect of flow rate, vortex finder depths, air core and particle interaction and described the performance of a deoiling hydrocyclone for variable flow rates. Neesse and Dueck [24] studied air core formation in the hydrocyclone and reported that air is often the neglected third phase of the 3-phase flow in the hydrocyclone. Martignoni et al. [25] studied the effect of cyclone geometry through the creation of a symmetrical inlet and a volute scroll outlet section experimentally and made comparisons with ordinary single tangential inlet cyclone. Ovalle et al. [26] studied the role of some wavelike motion observed in the interior of a conical hydrocyclone used in mineral processing operations and obtained a stable numerical solution of the equations of motion, using a stream function-vorticity formulation on a non-structured mesh. Cullivan et al. [27] studied numerically and validated experimentally the flow field of a 2 in. hydrocyclone shown to be significantly asymmetric without precession. Streamline expansion over the vortex-finder tip combined with existing secondary flow structure, established a globally static asymmetry throughout the hydrocyclone. Hence, the air-core predicted to exhibit a static asymmetry without precession, as was observed through high-speed video and radiography. Chinéand Concha [28] used a Laser Doppler Velocimeter, to determine the tangential and axial velocity fields for the water flow in a 102-mm modular hydrocyclone. R. Gupta et al. [3] studied experimentally the effect of air-core on the pressure across the hydrocyclone geometry. Due to the low pressure at the hydrocyclone axis, a back-flow of gas can occur then forms a gas-core. This gas-core affects the separation efficiency.

The objective of this paper is to numerically demonstrate the performance of a deoiling hydrocyclone and detect the effect of volume fraction of the two (liquid) phases on the cyclone separation efficiency.

2. Numerical details

2.1. Grid Generation and Meshing

In the present work numerical solution will be used for presenting the effect of variable volume fractions on the static pressure, axial, radial, tangential velocities and separation efficiency by using the RNG k-ε model for 2-phase liquid-liquid hydrocyclone. Water liquid was used as phase 1 and Crude oil was used as phase 2. The hydrocyclone was modelled by the commercial CFD code Fluent 6.3.26. This code uses the finite volume method. Mesh was structured by Gambit 2.3.16 with grid number of cells is 111373 and all cells were only hexahedral elements as shown in Figure (1-a, b).

TABLE1: SOLVER AND MESHING FEATURES USED IN THE CASE STUDY

Component of the hydrocyclone	Measurements (cm)
Internal diameter of the cylinder	10.0
Length of cylindrical portion	21.6
Length of the conical portion	36.5
Diameter of the underflow pipe	2.5
Diameter of the vortex finder pipe	1.8
The feed inlet dimensions	2.5 × 2.5
Vortex finder depth	12.5

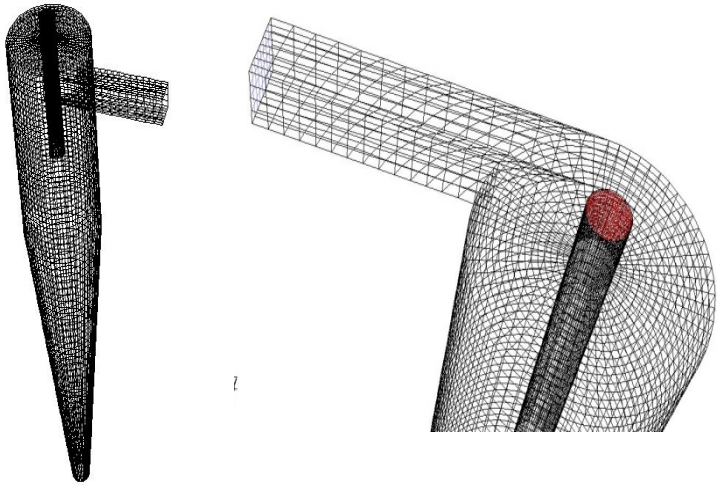

(a) (b)

Figure 1. Mesh shape.

2.2. Governing equations

The volume fraction of each phase is calculated from the continuity equation:

$$\frac{1}{\rho_{rq}}\left(\frac{\partial}{\partial t}(\alpha_q\rho_q)+\nabla\cdot(\alpha_q\rho_q\vec{v}_q)=\sum_{p=1}^{n}(\dot{m}_{pq}-\dot{m}_{qp})\right) \quad (1)$$

The solution of this equation for each phase, along with the condition that the volume fractions sum to one, allows for the calculation of the primary-phase volume fraction. This treatment is common to fluid-fluid and granular flows. Also the conservation of momentum for a fluid phase q reads:

$$\frac{\partial}{\partial t}(\alpha_q\rho_q\vec{v}_q)+\nabla\cdot(\alpha_q\rho_q\vec{v}_q\vec{v}_q)=-\alpha_q\nabla p+\nabla\cdot\bar{\bar{T}}_q+\alpha_q\rho_q\vec{g}+\sum_{p=1}^{n}\left(K_{pq}(\vec{v}_p-\vec{v}_q)+\dot{m}_{pq}\vec{v}_{pq}-\dot{m}_{qp}\vec{v}_{qp}\right)+(\vec{F}_q+\vec{F}_{lift,q}+\vec{F}_{vm,q}) \quad (2)$$

In the Euler-Euler approach, the different phases are treated mathematically as interpenetrating continua. For fluid-fluid multiphase flows, the transport equations for the present model are:

$$\frac{\partial}{\partial t}(\rho k)+\frac{\partial}{\partial x_i}(\rho k u_i)=\frac{\partial}{\partial x_j}\left[\alpha_k\mu_{eff}\frac{\partial k}{\partial x_j}\right]+G_k+G_b-\rho\varepsilon-Y_M+S_k \quad (3)$$

And

$$\frac{\partial}{\partial t}(\rho\varepsilon)+\frac{\partial}{\partial x_i}(\rho\varepsilon u_i)=\frac{\partial}{\partial x_j}\left[\alpha_\varepsilon\mu_{eff}\frac{\partial\varepsilon}{\partial x_j}\right]+C_{1\varepsilon}\frac{\varepsilon}{k}(G_k+C_{3\varepsilon}G_b)-C_{2\varepsilon}\rho\frac{\varepsilon^2}{k}+S_\varepsilon \quad (4)$$

The RNG K-ε model is derived using a rigorous statistical technique (called renormalization group theory). It is similar in form to the standard K-ε model, but includes the following refinements:

The RNG model has an additional term more than the standard model in its ε equation that significantly improves the accuracy for rapidly strained flows. The effect of swirl on turbulence is included in the RNG model, enhancing accuracy for swirling flows. The RNG theory provides an analytical formula for turbulent Prandtl numbers, while the standard K-ε model uses user-specified, constant values. While the standard K- ε model is a high-Reynolds-number model. The RNG theory provides an analytically-derived differential formula for effective viscosity that accounts for low-Reynolds-number effects. Effective use of this feature depends on an appropriate treatment of the near-wall region.

The scale elimination procedure in RNG theory results in a differential equation for the turbulent viscosity as:

$$d\left(\frac{\rho^2 k}{\sqrt{\varepsilon\mu}}\right) = 1.72\frac{\hat{\nu}}{\sqrt{\hat{\nu}^3 - 1 + C_\nu}}d\hat{\nu} \quad (5)$$

Where $\hat{\nu} = \mu_{eff}/\mu$. (6),

For accurate description of how the effective turbulent transport varies with the effective Reynolds number (or eddy scale), allowing the model to better handle low-Reynolds-number and near-wall flows.

In the high-Reynolds-number limit, Equation (5) gives

$$\mu_t = \rho C_\mu \frac{k^2}{\varepsilon} \quad (7)$$

These features make the RNG K-ε model more accurate and reliable for a wider range of flows than the standard K-εmodel.

The description of multiphase flow as interpenetrating continua incorporates the concept of phase volume fractions, denoted here by α_q. Volume fractions represent the space occupied by each phase, and the laws of conservation of mass and momentum are satisfied by each phase individually. The derivation of the conservation equations can be done by collective averaging the local instantaneous balance for each of the phases or by using the mixture theory approach.

The volume of phase q, V_q, is defined by

$$V_q = \int_V \alpha_q dV \quad (8)$$

Where

$$\sum_{q=1}^{n} \alpha_q = 1 \quad (9)$$

The effective density of phase q is given by

$$\hat{\rho}_q = \alpha_q \rho_q \quad (10)$$

$$Re = \frac{\rho V D_h}{\mu} \quad (11)$$

$$D_h = \frac{4A}{P} = \frac{4r^2}{4r} = r \quad (12)$$

The separation efficiency, η, is defined by:

$$\eta = \frac{\text{flow rate of phase 2 at upper outlet } (Q_{phase\,2})}{\text{total flow rate at inlet } (Q_{phase\,1} + Q_{phase\,2})} \quad (13)$$

3. Results and discussion

The results simulating the pressure and velocity fields inside the cyclone for different volume fractions (0.2, 0.4, 0.6, and 0.8) at different test runs are given below. The simulation studies are carried out using RNG k–ε model, Eulerian–Eulerian approach model by using Fluent 6.3.26

commercial software. These simulations were done at a constant velocity feed equals 2 m/s., for water as phase1 and crude oil as phase2.

TABLE2: CHARECTERISTICS OF FLOW AT DIFFERENT VOLUME FRACTIONS

V_f	0.2	0.4	0.6	0.8
ρ (kg/m^3)	972	944	916	888
$\mu \times 10^{-3}$ (kg/m.s)	2.42	3.84	5.26	6.68
Re	20082.64	12291.67	8707.224	6646.707

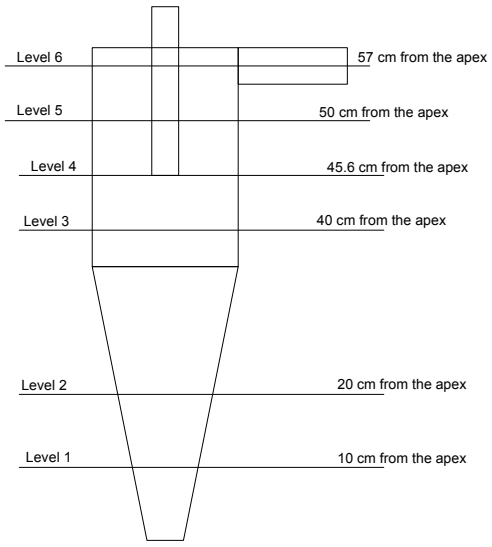

Figure 2. Computation levels.

Six levels in the hydrocyclone are considered as shown in Figure (2). Results will be focused on levels 2, 3, 5.The following legend signs are used:
(■) For volume fraction 0.2, (♦) for volume fraction 0.4, (▲) for volume fraction 0.6, and (●) for volume fraction 0.8. Also; (———) for phase 1 and (·····) for phase 2.The axial coordinate represents the dimensionless radius r/R and the vertical coordinate represents the dimensionless parameter.

Simulated general flow patterns in the cyclone in terms of static pressures and axial, radial and tangential velocities are shown in Figure 3 (a, b, c, d, respectively). Figure 4 (a, b, c) demonstrates computational results of non-dimensional static pressure variation with radial distance at levels 2, 3 and 5, respectively. The corresponding non-dimensional variation of axial, radial and tangential velocity components are shown in Figs. 5(a,b,c), 6(a,b,c) and 7(a,b,c), respectively.

Figure3-a illustrates the variation of static pressure through the hydrocyclone. The pressure decreases through the finder because of fluid suction; also it increased at the hydrocyclone sides because of high swirl, and in (figure 3-b) shows the direction of flow across the hydrocyclone according to axial velocity which is down at the sides and up for the interior.

In (figure 3-c) the flow has zero velocity at the sides and max. at the centre and different direction because of rotation. From (figure 3-d) the tangential velocities get its max. value in the conical section and increases during the cylindrical part.

In (figure 4- a, b, c)static pressure increases by increasing the volume fraction in all levels. This occurs because of lowering of the overall density, which increases the velocity. These results are largely in agreement with those reported by Bhaskar et al, 2006 [12].

Axial velocity generally increases by increasing the volume fraction in all levels (figure 5- a, b, c). But it can be noticed that axial velocity of phase 1 is less than that of phase 2. The difference decreases to become unnoticed for high levels at the top, due to high swirl velocity. Again, these results are in line with those observed by Bhaskar et al, 2006 [12].

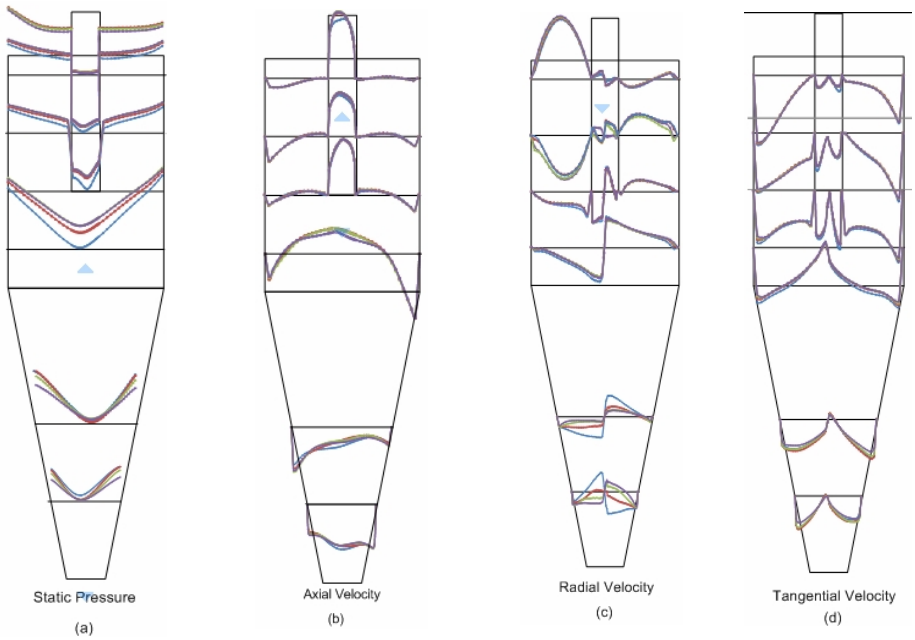

Figure 3. Non-dimensional Variation of static pressure and velocity components with radial distance at different levels inside cyclone.

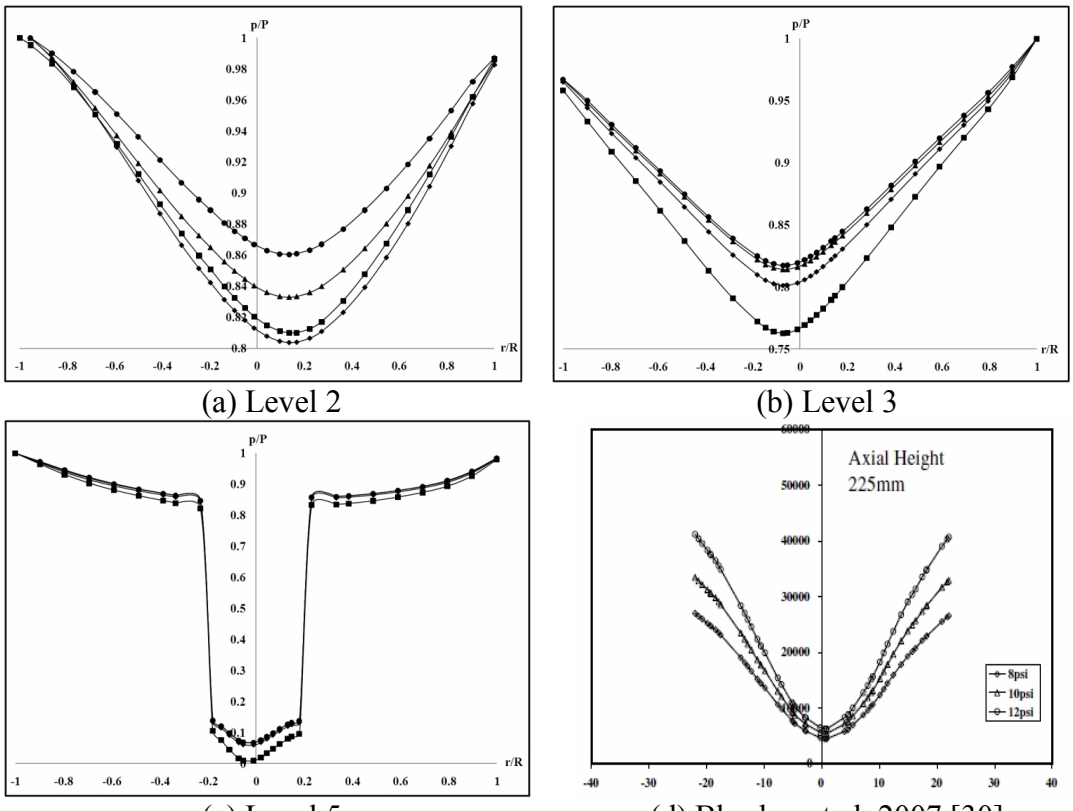

(a) Level 2 (b) Level 3

(c) Level 5 (d) Bhaskar et al, 2007 [30]

Figure 4. Static pressure

Radial velocity, increases by increasing the volume fraction in all levels (figure 6- a, b, c). But it can be noticed that radial velocity of phase 2 is less than phase 1.Results in fig 6-d represent the tangential velocity; which resembles in behaviour, with some difference, the radial velocity. This difference could be due to differences at coordinates.

For tangential velocity, the difference between the volume fraction values is very small as shown in (figure 7- a, b, c).

Finally, the efficiency of the presented hydrocyclone increases by increasing the volume fraction. With the increase of volume fraction we see that the partial separation efficiency of phase-1 increases but that of phase-2 decreases. This is believed to occur due to high radial forces that make remixing at finder outlet.

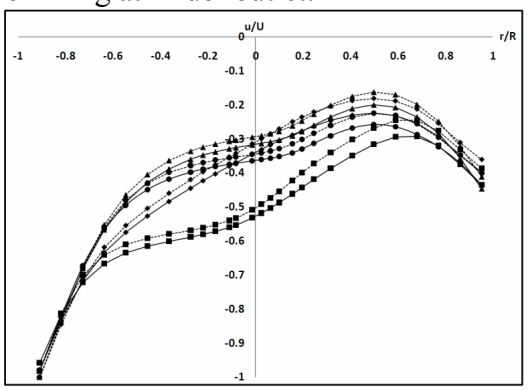

(a) Level 2

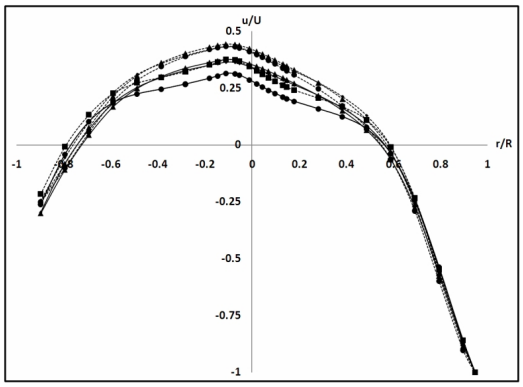

(b) Level 3

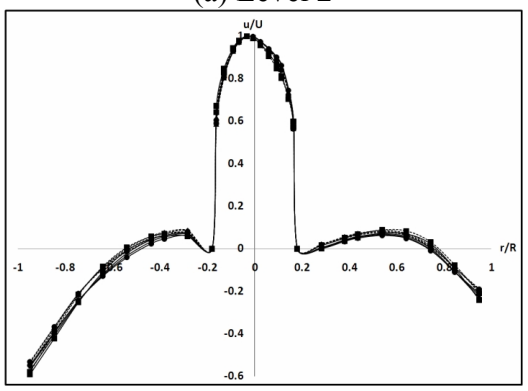

(c) Level 5

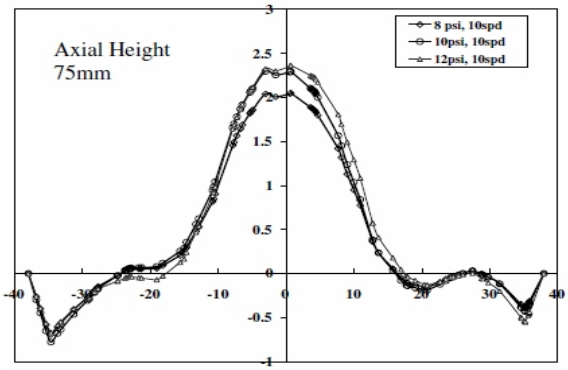

(d) Bhaskar et al, 2007 [30]

Figure 5. Axial velocity

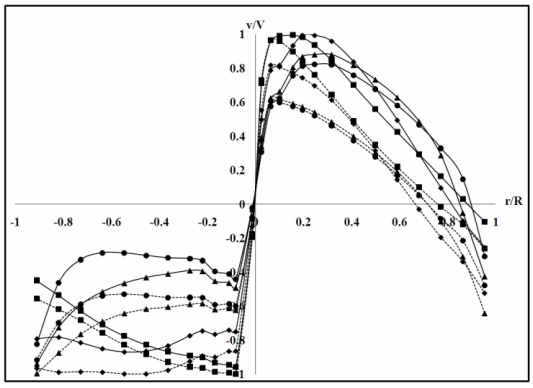

(a) Level 2

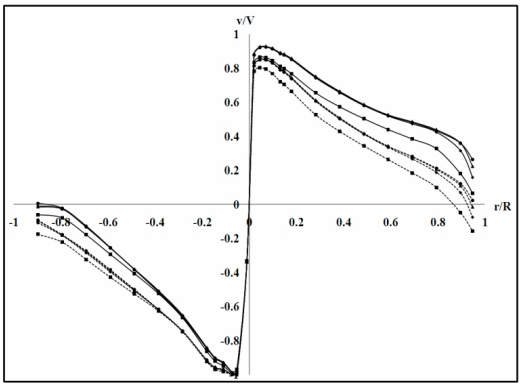

(b) Level 3

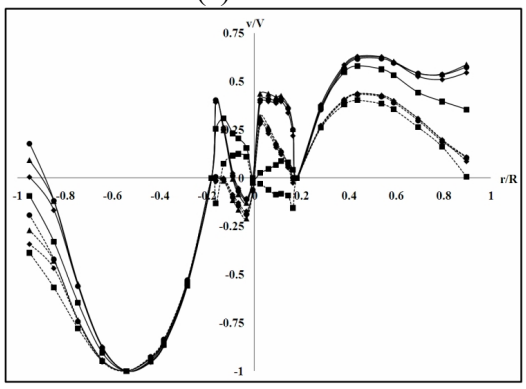

(c) Level 5

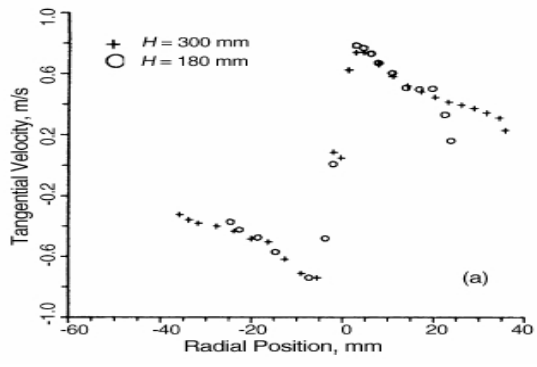

(d) Bergström and Vomhoff, 2007 [2]

Figure 6. Radial velocity

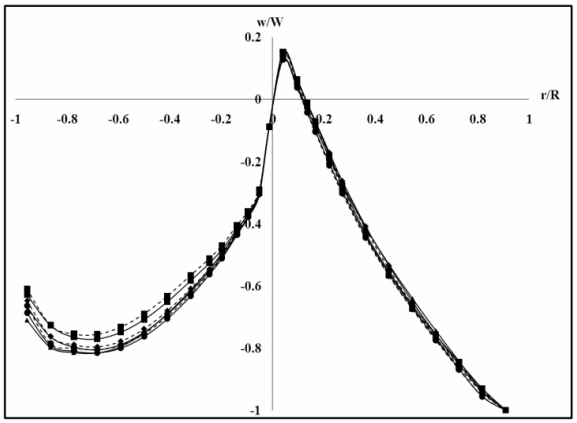

(a) Level 2

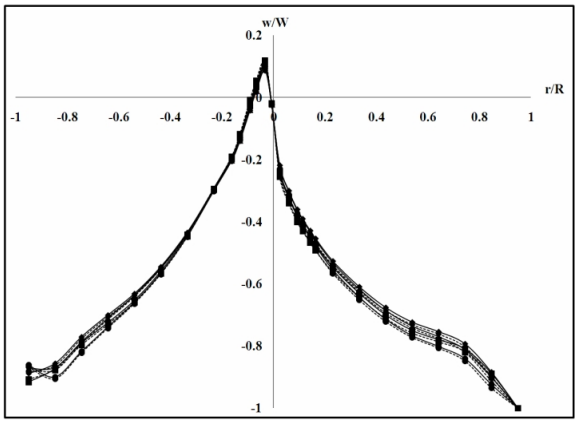

(b) Level 3

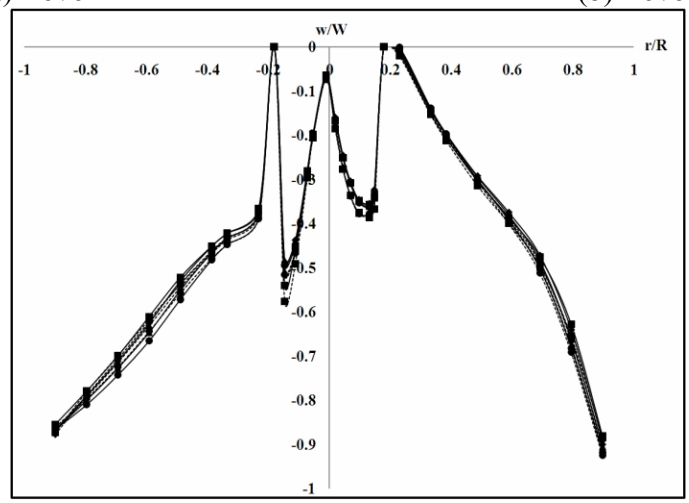

(c) Level 5

Figure 7. Tangential velocity

4. Conclusions

In hydrocyclones used for separation of two liquid phases, with increase of volume fraction:

- The static pressure and both axial and radial velocities all increase upward in the conical section up till the entrance of the cyclone finder.
- Relatively slight changes in the above parameters occur from the finder entrance to the top of the hydrocyclone.
- Small changes are resulted in tangential velocity values across the hydrocyclone.
- The separation efficiency increases, although it has in general relatively small values.
- The partial separation efficiency of phase 1 increases whereas that of phase 2 decreases.

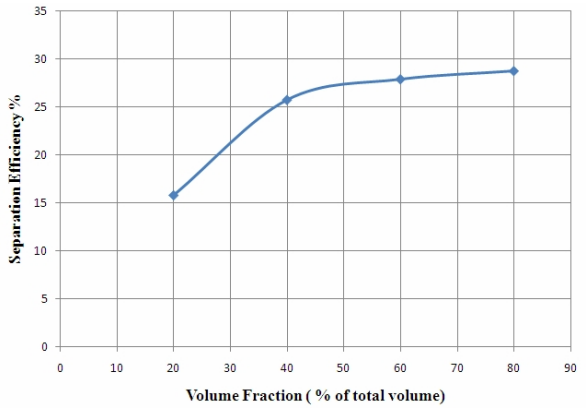

Figure 8. Variation of separation efficiency with volume fraction

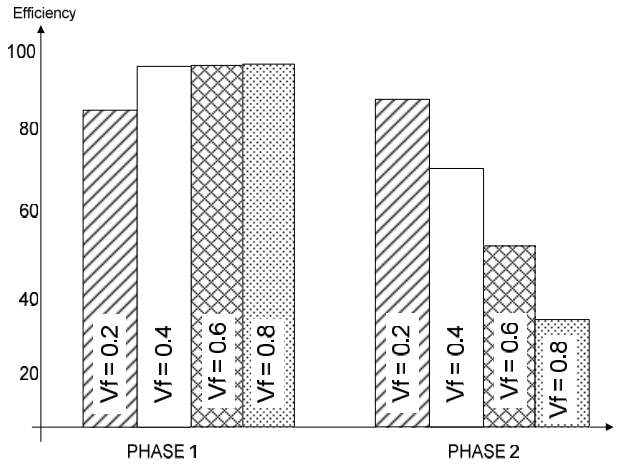

Figure 9.Partial separation efficiency for different volume fractions.

Nomenclature

A	Area.
C	Drag coefficient.
$C_{1\varepsilon}$, $C_{2\varepsilon}$ and $C_{3\varepsilon}$	Constants.
D_h	Hydraulic diameter (m).
F_D	Drag force, (N).
$\vec{F}_{lift,q}$	Lift Force, (N).
$\vec{F}_q$	External body Force, (N).
$\vec{F}_{vm,q}$	Virtual mass force, (N).
$\vec{g}$	Gravitational acceleration, (m/s^2).
G_k	Generation of turbulent kinetic energy due to the mean velocity gradient.
G_b	Generation of turbulent kinetic energy due to buoyancy.
K	Turbulent kinetic energy, (N.m).
P	Perimeter, (m).
Re	Reynolds Number.
S_k and S_ε	User-defined source terms.
t	Time, (s).
$\bar{\bar{T}}_q$	Phase stress – stress tensor, (Pa).
U	Axial velocity, (m/s).
V	Radial velocity, (m/s).
W	Tangential velocity, (m/s).
Y_M	Contribution of the fluctuating dilatation in compressible turbulence to the overall dissipation rate
α_k and α_ε	The inverse effective Prandtl numbers for k and ε, respectively.
ε	Dissipation rate of the turbulent kinetic energy, (m^2/s^3).
η	Separation efficiency
μ	Molecular viscosity of the fluid, (Pa.s).
μ_t	Turbulent eddy viscosity, (Pa.s).
ρ_q	Physical density of phase q, (kg/m^3).
ρ_{rq}	Phase reference density, (kg/m^3).

σ_k and σ_ε	Turbulent Prandtl numbers for k and ε.
Abbreviations:	
CFD	Computational Fluid Dynamics.
LES	Large Eddy Simulation.
RNG	Renormalization Group Method.
RSM	Reynold's Stress Model.

References

[1] Trygve Husveg, Odile Rambeau, Tormod Drengstig, Torleiv Bilstad, "Performance of a Deoiling Hydrocyclone during Variable Flow Rates". Minerals Engineering, 2007, Vol. 20, PP. 368–379.

[2] Jonas Bergström and Hannes Vomhoff, "Experimental Hydrocyclone Flow Field Studies". Separation And Purification Technology, 2007, Vol. 53, PP. 8–20.

[3] R. Gupta, M.D. Kaulaskar, V. Kumar, R. Sripriya, B.C. Meikap, S. Chakraborty, "Studies On The Understanding Mechanism Of Air Core And Vortex Formation In A Hydrocyclone". Chemical Engineering Journal, 2008, Vol. 144, PP. 153–166.

[4] Sina Amini, Dariush Mowlaa, Mahdi Golkar, Feridun Esmaeilzadeh, "Mathematical Modeling of a Hydrocyclone for the Down-Hole Oil–Water Separation (DOWS)". Chemical Engineering Research and Design, 2012, Vol. 90, PP. 2186–2195.

[5] Liu Hai-Fei, XU Jing-Yu, ZHANG Jun, SUN Huan-Qiang, ZHANG Jian, WU Ying-Xiang, "Oil/Water Separation in a Liquid-Liquid Cylindrical Cyclone". Journal of Hydrodynamics, 2012, Vol.24, No. 1, PP.116-123, DOI: 10.1016/S1001-6058(11)60225-4.

[6] Kuo-Jen Hwang, Ya-Wen Hwang, Hideto Yoshida, Kazuha Shigemori, "Improvement of Particle Separation Efficiency by Installing Conical Top-Plate in Hydrocyclone". Powder Technology, 2012, Vol. 232, PP. 41–48.

[7] Lian-Ze Wang and Ji-Ming Wang, "Experimental Study of the Drag Reduction and Separation Efficiency for a New Hydrocyclone with a Reducing Pressure Drop Stick". Separation And Purification Technology, 2012, Vol. 98, PP. 7–15.

[8] Sina Amini, Dariush Mowla, Mahdi Golkar, "Developing a New Approach for Evaluating A De-Oiling Hydrocyclone Efficiency". Desalination, 2012, Vol. 285, PP.131–137.

[9] R.Q. Honaker, A.V. Ozsever, N. Singh Ii and B.K. Parekh. "Apex Water Injection for Improved Hydrocyclone Classification Efficiency". Minerals Engineering, 2001, Vol. 14, No 11, PP. 1445-1457.

[10] Sonali Swain and Swati Mohanty, "A 3-Dimensional Eulerian–Eulerian CFD Simulation of a Hydrocyclone". Applied Mathematical Modeling, 2013, Vol. 37, PP. 2921–2932.

[11] M. Narasimha, Mathew Brennan, P.N. Holtham, "Large Eddy Simulation of Hydrocyclone Prediction of Air-Core Diameter and Shape". Int. J. Miner. Process, 2006, Vol. 80, PP. 1–14.

[12] K. Udaya, Y. Rama Murthy, M. Ravi Raju, Sumit Tiwari, J.K. Srivastava and N. Ramakrishnan, "CFD Simulation and Experimental Validation Studies on Hydrocyclone". Minerals Engineering, 2007, Vol. 20, PP. 60–71.

[13] LU Yaojun, ZHOU Lixing and SHEN Xiong, "Numerical Simulation of Strongly Swirling Turbulent Flows in a Liquid-Liquid Hydrocyclone Using the Reynolds Stress Transport Equation Model". Science in China, February, 2000, Series E, Vol. 43, No. 1.

[14] M. Karimi, G. Akdogan, K.H. Dellimore, S.M. Bradshaw, "Quantification of Numerical Uncertainty in Computational Fluid Dynamics Modeling of Hydrocyclones". Computers and Chemical Engineering, 2012, Vol. 43, PP. 45– 54.

[15] Chaiyaporn Puprasert, Vorasiri Siangsanung, Christelle Guigui, Céline Levecqc, Gilles Hébrard, "Hybrid Hydrocyclone Process Operating With Natural Water". Chemical Engineering And Processing, 2012, Vol. 61, PP. 8– 15.

[16] Lixin Zhao, Minghu Jiang, Baorui Xu, Baojun Zhu, "Development of a New Type High-Efficient Inner-Cone Hydrocyclone". Chemical Engineering Research And Design, 2012, Vol. 90, PP. 2129–2134.

[17] Okan Topcu, "CFD-DP Modeling of Multiphase Flow in Dense Medium Cyclone". CFD Letters, 2012, Vol. 4, No. 1.

[18] Shi Shi-Ying, Xu Jing-Yu, Sun Huan-Qiang, Zhang Jian, Li Dong-Hui, Wu Ying-Xiang, "Experimental Study of a Vane-Type Pipe Separator for Oil–Water Separation". Chemical Engineering Research and Design, 2012, Vol. 90, PP. 1652–1659.

[19] WANG Hualin, ZHANG Yanhong, WANG Jiangang and LIU Honglai, "Cyclonic Separation Technology: Researches and Developments". Chinese Journal of Chemical Engineering, 2012, Vol. 20, No. 2, PP. 212 – 219.

[20] Y. Rama Murthy and K. Udaya Bhaskar, "Parametric CFD Studies On Hydrocyclone". Powder Technology, 2012, Vol. 230, PP. 36–47.

[21] GAO Shu-Ling, WEI De-Zhou, LIU Wen-Gang, MA Long-Qiu, LU Tao, ZHANG Rui-Yang "CFD Numerical Simulation ofFlow Velocity Characteristics of Hydrocyclone". Transaction ofNonferrous Metals, Society of China, 2011, Vol. 21, PP.2783-2789.

[22] Jose A. Delgadillo and Raj K. Rajamani, "Exploration of hydrocyclone designs using computational fluid dynamics" Int. J. Miner. Process, 2007, Vol. 84, PP. 252–261.

[23] R. Sripriya, M.D. Kaulaskar, S. Chakraborty, B.C. Meikap, "Studies on The Performance of a Hydrocyclone and Modeling for Flow Characterization in Presence and Absence of Air Core". Chemical Engineering Science, 2007, Vol. 62, PP. 6391 – 6402.

[24] T. Neesse and J. Dueck, "Air Core Formation In The Hydrocyclone". Minerals Engineering, 2007, Vol. 20, PP. 349–354.

[25] W. P. Martignoni, S. Bernardo and C. L.Quintani, "Evaluation of Cyclone Geometry and Its Influence on Performance Parameters by Computational Fluid Dynamics (CFD)". Brazilian Journal Of Chemical Engineering, January - March, 2007, Vol. 24, No. 01, Pp. 83 – 94.

[26] E. Ovalle, R. Araya, F. Concha, "The Role of Wave Propagation in Hydrocyclone Operations I: An axisymmetric Stream Function Formulation for a Conical Hydrocyclone". Chemical Engineering Journal, 2005, Vol. 111, PP. 205–211.

[27] J.C. Cullivan, R.A. Williams, T. Dyakowski, C.R. Cross, "New Understanding of a Hydrocyclone Flow Field and Separation Mechanism from Computational Fluid Dynamics". Minerals Engineering, 2004, Vol. 17, PP. 651–660.

[28] B. Chine and F. Concha, "Flow Patterns In Conical and Cylindrical Hydrocyclones". Chemical Engineering Journal, 2000, Vol. 80, PP. 267.

[29] Wu Chen, Nathalie Zydek, Frank Parma, "Evaluation of Hydrocyclone Models For Practical Applications". Chemical Engineering Journal, 2000, Vol. 80, PP. 295–303.

[30] K. Udaya Bhaskar, Y. Rama Murthy, M. Ravi Raju, Sumit Tiwari, J.K. Srivastava b, N. Ramakrishnan, "CFD simulation and experimental validation studies on hydrocyclone". Minerals Engineering, 2007, Vol. 20, PP. 60–71.